Paleoceanography and Paleoclimatology

RESEARCH ARTICLE
10.1029/2020PA003890

Compound-Specific Radiocarbon Analysis of (Sub-) Antarctic Coastal Marine Sediments—Potential and Challenges for Chronologies

S. Berg[1], S. Jivcov[1], S. Kusch[2], G. Kuhn[3], L. Wacker[4], and J. Rethemeyer[1]

[1]Institute of Geology and Mineralogy, University of Cologne, Cologne, Germany, [2]Department of Prehistoric Archaeology, University of Cologne, Cologne, Germany, [3]Alfred Wegener Institute (AWI), Helmholtz Centre for Polar and Marine Research, Bremerhaven, Germany, [4]Ion Beam Physics, ETH Zurich, Switzerland

Abstract In Antarctic and Subantarctic environments, ^{14}C-based age determination is often challenging due to unknown reservoir effects, low organic carbon contents of sediments, and high contributions of petrogenic (^{14}C-free) carbon in ice marginal settings. In this study, we evaluate possible benefits and challenges of compound-specific radiocarbon analysis (CSRA) as a tool for age determination of marine Antarctic and Subantarctic sediment sequences. We present a comprehensive data set of ^{14}C ages obtained on bulk organic carbon, carbonates, and on fatty acids (FA) from three coastal marine sediment cores from Subantarctic South Georgia and East Antarctica. Low molecular weight (LMW) FA represent the least ^{14}C-depleted fraction, indicating that the phytoplankton-derived compounds can be a means of dating sediments. In contrast, vascular plant-derived high molecular weight FA are systematically depleted in ^{14}C relative to the low molecular weight homologues, reflecting processes such as soil formation/erosion in the catchment. Comparative age-depth models show significant differences, depending on the material used for the respective models. While the land plant-derived FA may lead to an overestimation of the actual sediment age, LMW FA reveal complex aquatic reservoir effects. Bulk sedimentary organic carbon ^{14}C ages likely provide appropriate age estimates in settings with low petrogenic carbon input in the Antarctic, whereas CSRA has the potential to produce improved age control in settings with high contributions of petrogenic carbon.

Key Points:
- Phytoplankton-derived low molecular weight fatty acids can be used to date Antarctic marine sediments
- Contribution of petrogenic, reworked carbon in Antarctic and Subantarctic shelf settings can be assessed by compound-specific radiocarbon analysis
- Land plant-derived high molecular weight fatty acids in the Subantarctic are systematically depleted in radiocarbon

Supporting Information:
- Supporting Information S1

Correspondence to:
S. Berg,
sberg0@uni-koeln.de

Citation:
Berg, S., Jivcov, S., Kusch, S., Kuhn, G., Wacker, L., & Rethemeyer, J. (2020). Compound-specific radiocarbon analysis of (sub-)Antarctic coastal marine sediments—Potential and challenges for chronologies. *Paleoceanography and Paleoclimatology*, *35*, e2020PA003890. https://doi.org/10.1029/2020PA003890

Received 20 FEB 2020
Accepted 15 SEP 2020
Accepted article online 24 SEP 2020

1. Introduction

Radiocarbon dating is the most widely used method for age determination of sedimentary records for the Late Pleistocene and Holocene period (<55,000 years). In general, the ^{14}C isotopic composition of organic matter (OM) and carbonates reflects the ^{14}C isotopic composition of the primary carbon pool utilized by the respective organisms. While terrestrial OM mostly forms in equilibrium with atmospheric ^{14}C, reservoir effects often impede a simple interpretation of sedimentary ^{14}C ages in aquatic environments (marine and lacustrine, e.g., Gordon & Harkness, 1992; Hendy & Hall, 2006; Moreton et al., 2004). In the Southern Ocean, sea ice cover and more importantly regional upwelling of deep-water masses lead to reservoir ages of on average 1,100–1,300 years (e.g., Berkman & Forman, 1996). Surface water reservoir ages may change regionally over time due to changes in oceanography and freshwater influx from the continent (e.g., Hall et al., 2010; van Beek et al., 2002). Estimation of reservoir ages is particularly difficult in isolated basins and marine inlets in coastal areas, which are influenced by changing marine and freshwater contributions. However, records from these areas are important for relative sea level reconstructions and provide information on climate and glaciation histories (e.g., Berg, White, Jivcov, et al., 2019; Hodgson et al., 2016).

In marine sediments, carbonate fossils like foraminifer tests are frequently used for reconstructing sediment ages (e.g., Graham et al., 2017). However, across the Southern Ocean, carbonates are poorly or not at all preserved in the sediments and ^{14}C analysis of bulk sedimentary organic carbon (OC) is often used for age determination (e.g., Hillenbrand et al., 2009). In surface sediments of the Southern Ocean, ^{14}C ages of bulk OC often exceed the marine reservoir age reflecting the admixture of petrogenic or reworked OC, especially in settings close to ice sheets and glaciers and/or when autochthonous primary production is low or organic matter is not well preserved (e.g., Andrews et al., 1999; Ohkouchi & Eglinton, 2006; Subt et al., 2017). In coastal areas of the Subantarctic, organic matter derived from plants, soils, and peat deposits are

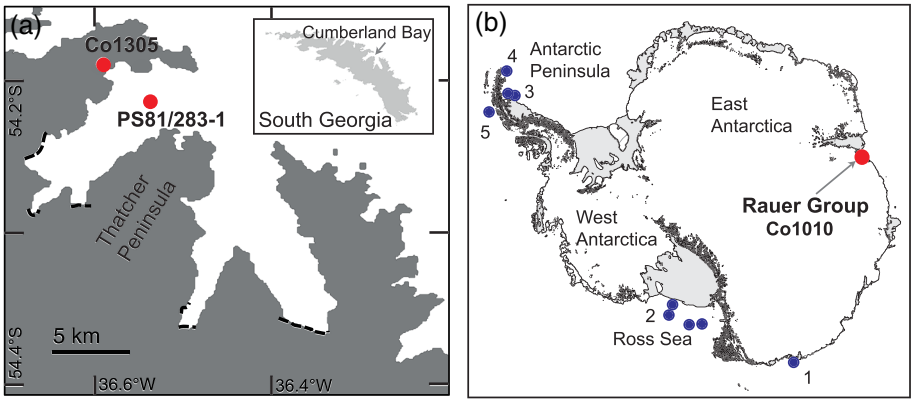

Figure 1. (a) Marine coring locations Co1305 (Berg, White, Jivcov, et al., 2019), and PS81/283-1 (Bohrmann, 2013) in Cumberland West Bay, South Georgia. Dashed lines indicate outlet glaciers terminating in Cumberland Bay. (b) Rauer Group, an ice-free coastal archipelago in East Antarctica. Numbers indicate sites of previous studies applying compound-specific and ramped pyrolysis ^{14}C analyses in Antarctic sediments: 1 Yamane et al. (2014); 2 Yokoyama et al. (2016), Ohkouchi and Eglinton (2008); 3 Subt et al. (2017); 4 Rosenheim et al. (2008); 5 Rosenheim et al. (2013).

additional OC sources (Berg, White, Jivcov, et al., 2019). Several studies showed that terrestrial OC deposited in marine sediments is often considerably ^{14}C-depleted upon deposition, which reflects the input of material stored for decades to thousands of years on land prior to transport into the ocean (e.g., Drenzek et al., 2007; Kusch et al., 2010; Schefuß et al., 2016; Vonk et al., 2014; Winterfeld et al., 2018). The ^{14}C ages of terrestrial OC are controlled by many variables such as climatic conditions, vegetation and soil type, morphology and geology of the drainage areas (e.g., Cui et al., 2017; Drenzek et al., 2007; Kusch et al., 2010; Vonk et al., 2014). Evidence for these processes primarily comes from temperate regions or the Arctic, but thus far no studies investigate the degree of ^{14}C depletion of terrestrial OM in marine sediments in Subantarctic marine environments.

Different ^{14}C techniques have been developed to separate ^{14}C signatures of OC from different sources. For example, ramped pyrolysis (RP) employs sequential heating to release OC fractions from sediments based on their thermochemical stability allowing for the quantification of refractory and labile OC (e.g., Rosenheim et al., 2008, 2013). Compound-specific ^{14}C analysis (CSRA) separates individual organic molecules from sediments using preparative gas chromatography (PCGC) or high performance liquid chromatography (e.g., Eglinton et al., 1996; Ingalls & Pearson, 2005). For example, in the Ross Sea, Antarctica, CSRA of phytoplankton-derived low molecular weight (LMW) fatty acids (containing 14, 16, and 18 C atoms) in surface sediments has been shown to match the dissolved inorganic carbon (DIC) ^{14}C isotopic composition of the water column (e.g., Ohkouchi & Eglinton, 2008), while substantial contributions of petrogenic OC in sediments restrict meaningful age determination using bulk OC ^{14}C analysis (e.g., Andrews et al., 1999). This makes sedimentary LMW fatty acids (FA) primary targets for ^{14}C analysis to provide age information when carbonate microfossils are absent and contributions of petrogenic OC are suspected. A recent study by Yokoyama et al. (2016) presented first core chronologies of Ross Sea sediments based on CSRA of LMW FA, which aided a better understanding of ice shelf instability during the Holocene (Figure 1). However, despite the great potential of such data until now only few studies have used CSRA to improve age-depth models for Antarctic and Subantarctic marine sediments (Berg, White, Jivcov, et al., 2019; Ohkouchi & Eglinton, 2008; Yamane et al., 2014; Yokoyama et al., 2016, Figure 1).

In this study, we evaluate possible benefits and challenges of CSRA as a tool for age determination of marine Antarctic and Subantarctic sediment sequences. This way, we extend the regional CSRA database and aim at evaluating in which setting CSRA is particularly useful compared to dating of bulk OC and/or of discrete carbonate microfossils. Our study focuses on coastal marine environments, which are crucial sites for the reconstruction of ice dynamics and paleoclimatic conditions. We compare different records from East Antarctica and from the Subantarctic, which differ in their main carbon input sources (marine, petrogenic, terrestrial), in OC content (0.4% to 4%) and age of sedimentation (modern to late Pleistocene). As an end member for terrestrial OC we use high molecular weight (HMW) FA (24 to 34 C atoms), which derive mainly from

leaf waxes of higher terrestrial plants and are frequently used as markers for land-plant derived OM in marine sediments (e.g., Cui et al., 2017; Drenzek et al., 2007; Kusch et al., 2010; Vonk et al., 2014). We use LMW FA as ^{14}C end member for the autochthonous marine component. By using the respective terrestrial and aquatic end member $F^{14}C$ values, it is possible to estimate the proportion of petrogenic OC to bulk OC.

2. Study Areas and Sediment Cores

2.1. Subantarctic

The Subantarctic island of South Georgia (54–55°S, 36–38°W, Figure 1) is located north of the present-day winter sea ice margin. The mountainous interior of the island hosts ice fields and glaciers, some of which drain into the adjacent fjords. Core PS81/283-1 (36°32.280′W, 54°12.920′S) was recovered in Cumberland West Bay from a water depth of 193 m (Bohrmann, 2013). The coring site is located downstream of Neumayer Glacier (Figure 1), which releases meltwater and suspended and ice-rafted debris (IRD) into Cumberland West Bay (Geprägs et al., 2016; Graham et al., 2017). In Cumberland Bay extensive submarine cold-seep areas were discovered, where methane is emitted from sediments into the water column (Römer et al., 2014). Core PS81/283-1 comprises a 4.66 m long sediment section of fine-grained (fine to medium silt, on average sand 4 wt%, silt 63 wt%, clay (<2 μm) 33 wt%) bioturbated siliciclastic material with interspersed larger grains (average gravel content 3.2 wt%), which likely represent IRD.

Core Co1305, comprising an 11.04 m long sediment record, was recovered from a marine inlet (Little Jason Lagoon) (36°35.469′W, 54°11.568′S) on the northwestern shore of Cumberland West Bay (Figure 1). Little Jason Lagoon has a maximum water depth of 24 m and a sill at 0.5 to 1.5 m depth, which enables permanent water exchange with the fjord. The terrestrial catchment is presently free of permanent ice. However, several small streams enter the inlet and supply freshwater, for example, during snowmelt (White et al., 2018). The catchment has vegetation and soil coverage below 200 m altitude representing a likely source of OM to the sediments. Core Co1305 contains a glacial diamicton at the base that is overlain by lacustrine and marine deposits. Stable isotope and diatom assemblage data showed that the former lake transitioned into a marine inlet and was permanently in contact with marine waters since then (Berg, White, Hermichen, et al., 2019). The marine sediments are fine grained with some interspersed IRD, and carbon contents range from of 1.0 to 3.3 wt% (Figure 2). A comprehensive dataset of ^{14}C content values of bulk OC, carbonates, terrestrial plant fossils and $C_{16:0}$ FA indicates a Holocene age of the record (Berg, White, Jivcov, et al., 2019).

2.2. East Antarctica

Rauer Group (77°54′E, 68°48′S) is an archipelago to the East of Prydz Bay (Figure 1). The islands are presently free of permanent snow and ice and host some small, mostly saline lakes. The marine inlets between the islands are covered by sea ice during austral winter and some also retain an ice cover during summer. Sediments in these inlets are rich in OM and consist of diatom-rich sapropelic muds, while organic matter input from land is negligible (Berg et al., 2010). High sedimentation rates (in some cases exceeding 1 m per 1,000 years) have been reported from such marine inlets, for example, from East Antarctic oases like Bunger Hills (Berg et al., 2020) and Windmill Islands (Cremer et al., 2003). These sediments therefore provide high-resolution records of environmental changes in these remote regions. Core Co1010 was recovered from a marine inlet, ~4 km to the north of the sea-terminating ice sheet margin. Water depth at the coring location was 38 m, and a 21.4 m long section of marine sediments was recovered (Berg et al., 2010). The basal unit I (21.43 to 19.30 m depth) consists of diatomaceous mud and was assigned to the late Pleistocene based on bulk OC ^{14}C ages. The cryogenic texture and low water content of the sediments point to postdepositional freezing and likely compaction by an overlying ice sheet. The upper 19.30 m of the sequence reflect the post-glacial and Holocene sedimentation history of the inlet, which is characterized by clastic-rich deglacial sediments (unit II) and a diatom and OC-rich sapropel (OC 2–4 wt%) throughout the remainder of the Holocene (unit III, Figure 3, Berg et al., 2010).

3. Methods

3.1. Compound-Specific Radiocarbon Analysis

Samples for CSRA were obtained from up to 66 g freeze-dried sediments (Table S2 in the supporting information). For core Co1010, the total lipid extract (TLE) was obtained by ultrasonication. Samples

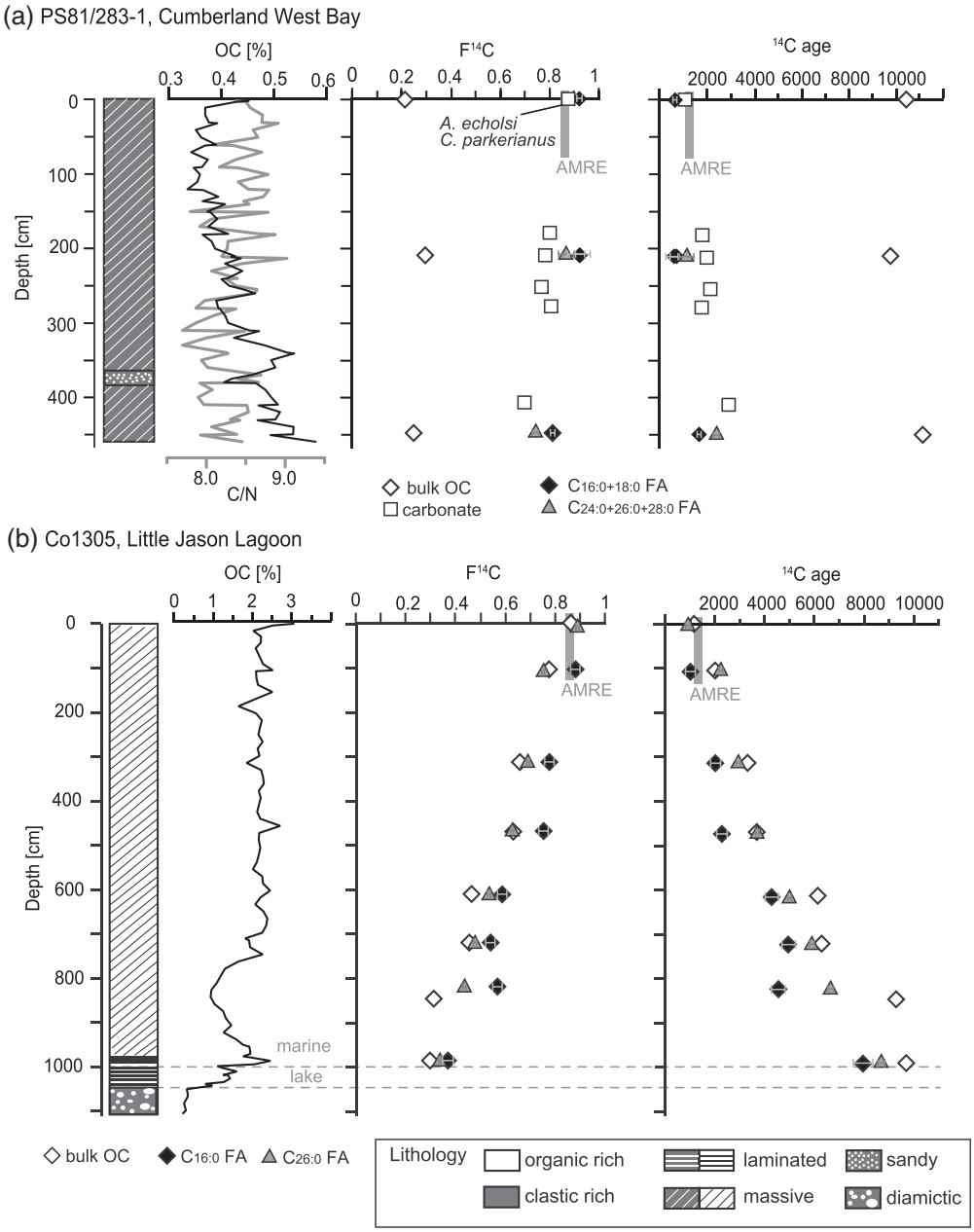

Figure 2. (a) Core PS81/283-1: Lithology, total organic carbon (OC) (wt%) and OC/N ratio, $F^{14}C$, and corresponding ^{14}C ages bulk OC, HMW ($C_{24:0}$ + $C_{26:0}$ + $C_{28:0}$), LMW ($C_{16:0}$ + $C_{18:0}$) FA, and carbonates. (b) Core Co1305: Lithology, total organic carbon (OC) (wt%), $F^{14}C$ and corresponding ^{14}C ages of bulk OC, HMW ($C_{26:0}$), and LMW ($C_{16:0}$) FA. Error bars represent 1σ uncertainties, error bars of bulk OC $F^{14}C$ values are well within the size of the symbols. $F^{14}C$ values of $C_{16:0}$ FA for core Co1305 are from Berg, White, Jivcov, et al. (2019). AMRE = Antarctic marine reservoir effect 1,100–1,300 years.

were extracted sequentially using methanol (MeOH), MeOH: dichloromethane (DCM) (1:1, v/v) and DCM: hexane (Hex) (1:1, v/v). The respective extracts were combined and desulfurized using activated copper. Samples of cores Co1305 and PS81/283-1 were extracted by accelerated solvent extraction (ASE 300, Thermo, USA) using DCM:MeOH (9:1, v/v at 120°C, 75 bar).

For purification of FA, the TLE was saponified with 0.5 M KOH in MeOH and water (9:1, v/v) at 80°C for 2 h. Neutral lipids were recovered from the TLE by liquid-liquid phase separation (DCM and water). Subsequently, the aqueous phase was acidified (pH 1) and the FA-fraction was extracted with DCM. FAs

were methylated with MeOH and concentrated hydrochloric acid (HCl) (95:5, v/v) at 80°C for 12 hr to form fatty acid methyl esters (FAMEs). FAMEs were further purified from other compounds by liquid-liquid phase extraction (Hex and water). To ensure separation of FAMEs from remaining non-methylated, polar compounds and water, FAMEs were eluted over an SiO_2-Na_2SO_4 column with DCM:Hex (2:1, v/v). Individual FA homologues were isolated using a 7,680 Agilent GC (7,680 Agilent Technologies, USA) equipped with a CIS 4 injection system (Gerstel, Germany) and coupled to a preparative fraction collector (PFC; Gerstel, Germany). Separation of individual FAs was achieved with a 30 m ultralow bleed fused-silica capillary column (film thickness 0.5 μm and 0.53 mm I. D, RTX-1, RESTEK). The FA fraction was dissolved in DCM and 5 μl were injected repeatedly (between 47 and 90 times, see Table S2 in the supporting information). The temperature program was 40 °C isothermal for 1 min, ramp to 220°C at a rate of 10°C/min, ramp to 320°C at a rate of 7°C/min, isothermal for 10 min. The PFC transfer line was heated constantly at 320°C. PFC glass traps (150 μl) were left at room temperature. Trapped compounds were flushed out of the traps with 1 ml DCM. The purity and quantity of isolated compounds was determined by GC-FID (Agilent 7890B, Agilent Technologies, USA) and compounds with purities >98% were processed further. Isolated compounds were combusted in vacuum-sealed quartz glass tubes and purified according to methods described in Rethemeyer et al. (2019), and the resulting CO_2 was analyzed using the MICADAS AMS system equipped with a gas ion source at the ETH Zurich (Wacker et al., 2010). Results are given in $F^{14}C$ (fraction modern carbon, Reimer et al., 2004) and conventional radiocarbon ages were calculated using conventions described in Stuiver and Pollach (1977).

The amount and isotopic composition of the processing blank (i.e., carbon introduced during sample handling, PCGC purification, and sealed tube combustion) was determined using C_{18} *n*-alkane (Fluka, Prod. No. 74691-5 g, Lot. 0001448903) with an $F^{14}C$ value of <0.0008 and squalane (C_{30} isoprenoid; Fluka, Prod. No. 85629-50 ml, Lot. 0001418796) with an $F^{14}C$ value of 1.0187 ± 0.0033. The total processing blank was quantified at 1.1 ± 0.6 μg C with an $F^{14}C$ value of 0.6088 ± 0.019 (Table S1). $F^{14}C$ values of the samples were corrected for blank addition and the addition of one methyl group added during transesterification ($F^{14}C_{MeOH} = 0.0008$) using mass balance, errors were propagated following Welte et al. (2018). Per convention, we consider $F^{14}C$ values insignificantly different when they agree within 2σ analytical uncertainty (95% confidence interval).

The mass of individual FAs ranged from 2 to 60 μg C (Table S2). For core PS81/283-1 LMW FA ($C_{16:0}$ and $C_{18:0}$) or HMW FA ($C_{24:0}$, $C_{26:0}$ and $C_{28:0}$) were each combined for CSRA, respectively, to obtain at least 5 μg C for ^{14}C analysis. From 211 cm core depth, LMW FA ($C_{16:0 + 18:0}$) were isolated and analyzed in duplicate to test the reproducibility of $F^{14}C$ values for samples <10 μg C (Table S2). Although values agree within 1σ analytical uncertainty (ETH-87515 5 μg C, $F^{14}C$ = 0.9210 ± 0.0462 and ETH-87516 (12 μg C, $F^{14}C = 0.9267 \pm 0.0184$; Table S2), we use the $F^{14}C$ value of the 12 μg C sample for age calculation and calibration due to the large error of the 5 μg sample.

3.2. Elemental and ^{14}C Analysis of Bulk Sediments and Carbonates

For cores Co1010 and Co1305, aliquots of each sediment sample were used for total organic carbon (OC) analysis using a DIMATOC 200 (DIMATEC Corp.). OC contents in core PS81/283-1 were determined after removal of the total inorganic carbon (TIC, carbonates) with HCl using an ELTRA CS2000. Total nitrogen (TN) was measured together with total carbon (TC) with an Elementar Vario EL III.

For bulk OC ^{14}C analysis, sediments of cores Co1010 and Co1305 were treated with HCl (0.5% and 1%) for 10 hr at room temperature to remove carbonates. Samples were washed with Milli-Q water (Millipore, USA) repeatedly and oven-dried at 60°C. For core PS81/283-1, a different protocol was used. Samples were treated with a standard acid-alkali-acid extraction to obtain humins, which are assumed to be representative for bulk OC (Rethemeyer et al., 2019). OC in the pretreated sediments was converted to graphite using an automated graphitization system (AGE) and analyzed at the CologneAMS facility.

Carbonate samples were wet-sieved and tests of foraminifer *Astrononion echolsi* and *Cassidulinoides parkerianus* were hand-picked from the >63 μm fraction. Cleaned foraminifers were analyzed at ETH Zurich with a recently developed method that allows measurements of small-size samples that contain only 0.3 to 1 mg carbonate (Bard et al., 2015). Samples were at first leached with 100 μl of 0.02 M HCl for cleaning to remove 100 μg carbonate in septa-sealed vials. The produced CO_2 of this step was also measured for quality control.

Then, the remaining sample material was measured after complete dissolution with 85% phosphoric acid. For the measurement, the produced CO_2 was directly introduced into an AMS using the gas ion source at the ETH Zurich (Wacker, Fahrni, et al., 2013; Wacker, Fülöp, et al., 2013). $F^{14}C$ values of the measured leach fractions were always close to the $F^{14}C$ values of the main fractions and thus confirm a good sample quality.

3.3. ^{14}C-Based Age-Depth Models

Age-depth models for the sediment records were developed with the software Clam 2.2 (Blaauw, 2010) by linear interpolation or polynomial regression based on unrounded ^{14}C ages. Terrestrial samples were calibrated using the SHcal13 data set (Hogg et al., 2013) and samples of marine origin were calibrated using the Marine13 data set (Reimer et al., 2013). Respective reservoir corrections are discussed in the text (section 5.4).

4. Results

4.1. PS81/283-1, Cumberland West Bay, South Georgia

OC contents in core PS81/283-1 range from 0.4 to 0.6 wt% (Figure 2). The C/N ratio of 67 samples is constant downcore with a mean of 8.3 ± 0.3 (1σ). Bulk OC ages were analyzed in three depths of core PS81/283-1. $F^{14}C$ values range from 0.296 ± 0.002 (9,780 ± 55 ^{14}C yr BP) to 0.250 ± 0.002 (11,140 ± 50 ^{14}C yr BP) but do not systematically change with depth (Table 1 and Figure 2a). In the uppermost sample (1–2 cm), benthic foraminifera yielded sufficient amounts for ^{14}C analysis. *A. echolsi*, an infaunal species (Dejardin et al., 2018), and the benthic *C. parkerianus* (Majevski, 2005) provided $F^{14}C$ values of 0.8751 ± 0.0062 (1,070 ± 60 ^{14}C yr BP) and 0.8743 ± 0.0049 (1,080 ± 50 ^{14}C yr BP), respectively (Table 1 and Figure 2a). At five greater core depths, carbonate mollusk shell debris was dated, that shows general ^{14}C-depletion with depth except for one reversal at 280 cm core depth (Table 1 and Figure 2a). $F^{14}C$ values range from 0.8007 ± 0.0046 (1,785 ± 45 ^{14}C yr BP) to 0.8698 ± 0.0039 (2,890 ± 45 ^{14}C yr BP) and are thus higher than $F^{14}C$ values for bulk OC. $F^{14}C$ values of $C_{16:0\ +\ 18:0}$ FA from 1–2 cm and from 211 cm are similar, 0.9228 ± 0.0099 (645 ± 85 ^{14}C yr BP) and 0.9267 ± 0.0184 (610 ± 160 ^{14}C yr BP), respectively (Figure 2a). $C_{16:0\ +\ 18:0}$ FA from the sample at 451 cm depth is more ^{14}C-depleted, with an $F^{14}C$ value of 0.8152 ± 0.0078 (1,640 ± 80 ^{14}C yr BP). Due to insufficient HMW FA concentrations, $F^{14}C$ values of HMW FA could not be obtained for the uppermost sample in core PS81/283-1. For 211 cm depth, combined HMW ($C_{24:0\ +\ 26:0\ +\ 28:0}$) FA provided an $F^{14}C$ value of 0.8790 ± 0.0325 (1,140 ± 300 ^{14}C yr BP) and at 451 cm depth HMW ($C_{24:0\ +\ 26:0\ +\ 28:0}$) FA were 0.7444 ± 0.0135 (2,370 ± 145 ^{14}C yr BP). The relatively large analytical uncertainties arise from the small sample sizes of some compounds (Table S2 in the supporting information).

4.2. Co1305, Little Jason Lagoon, South Georgia

A total of eight samples was analyzed from core Co1305. The $F^{14}C$ values of the bulk OC become successively more ^{14}C-depleted with depth ranging from 0.8620 ± 0.0040 (1,195 ± 35 ^{14}C yr BP) in the surface sample to 0.2995 ± 0.0024 (9,685 ± 65 ^{14}C yr BP) at 988 cm depth directly above the base of the marine sediment (Table 1 and Figure 2b). $F^{14}C$ values of $C_{26:0}$ FA agree with bulk OC for most of the investigated samples. Analogous to bulk OC, $F^{14}C$ values of $C_{26:0}$ FA become successively more ^{14}C-depleted with depth, ranging from 0.8932 ± 0.0114 (910 ± 105 ^{14}C yr BP) at 4–9 cm core depth to 0.3391 ± 0054 (8,690 ± 130 ^{14}C yr BP) at 988–993 cm depth (Figure 2b).

4.3. Co1010, Rauer Group, East Antarctica

In core 1,010, bulk OC of seven sediment samples was analyzed. The sample from the lowermost unit I provided an infinite age (not distinguishable from blank) corresponding to >52,000 ^{14}C yr BP (Table 1 and Figure 3). The $F^{14}C$ values for the upper units (II and III) decrease successively with depth, ranging from 0.7954 ± 0.0032 to 0.2940 ± 0.0015 (corresponding to 1,840 ± 30 to 9,840 ± 40 ^{14}C yr BP, Table 1 and Figure 3). For four of these samples, compound-specific ^{14}C data of FAs were obtained. The $C_{16:0}$ FA from 102–110 cm depth has a value of 0.8345 ± 0.0073 (1,445 ± 70 ^{14}C yr BP), which is less ^{14}C-depleted than the value for bulk OC from the same depth (Table 1). At 1,103–1,113 cm depth, $F^{14}C$ of the $C_{16:0}$ FA (0.4408 ± 0.0087; 6,580 ± 160 ^{14}C yr BP) is similar to the corresponding bulk OC value (0.4284 ± 0.002; 6,810 ± 35 ^{14}C yr BP). In the sample from unit II at 1,729 cm depth, $F^{14}C$ of the $C_{16:0}$ FA is 0.3419 ± 0.0122 (8,620 ± 285 ^{14}C yr BP) and thus higher than the corresponding bulk OC

Table 1
Results of ^{14}C Analysis for Bulk OC, Carbonates, and Fatty Acids and Terrestrial Plant Remains

Core	Depth (cm)	AMS lab ID	Dated material	$F^{14}C \pm 1\sigma$	^{14}C age (yr BP) $\pm 1\sigma$
Cumberland West Bay, South Georgia					
PS81/283-1	1–2	COL3055	bulk OC	0.2133 ± 0.0014	12,410 ± 50
		ETH-87286	*A. echolsi*	0.8751 ± 0.0062	1,070 ± 60
		ETH-87287	*C. parkerianus*	0.8743 ± 0.0049	1,080 ± 50
		ETH-80010	$C_{16:0 + 18:0}$ FA	0.9228 ± 0.0099	645 ± 85
	182	ETH-62118	carbonate	0.8007 ± 0.0046	1,785 ± 45
	211–212	COL3056	bulk OC	0.2960 ± 0.0017	9,780 ± 55
		ETH-87515	$C_{16:0 + 18:0}$ FA	0.9210 ± 0.0462	660 ± 405
		ETH-87516	$C_{16:0 + 18:0}$ FA	0.9267 ± 0.0184	610 ± 160
		ETH-87517	$C_{24:0 + 26:0 + 28:0}$ FA	0.8677 ± 0.0325	1,140 ± 300
	213	ETH-62119	carbonate	0.7828 ± 0.0043	1,970 ± 45
	255	ETH-62120	carbonate	0.7688 ± 0.0047	2,110 ± 50
	280	ETH-62121	carbonate	0.8046 ± 0.0046	1,746 ± 45
	410	ETH-62122	carbonate	0.6979 ± 0.0039	2,890 ± 45
	451–452	COL3057	bulk OC	0.2499 ± 0.0016	11,140 ± 50
		ETH-87519	$C_{16:0 + 18:0}$ FA	0.8152 ± 0.0078	1,640 ± 80
		ETH-87518	$C_{24:0 + 26:0 + 28:0}$ FA	0.7444 ± 0.0134	2,370 ± 145
Little Jason Lagoon, South Georgia					
Co1305	2–4	COL2894[a]	bulk OC	0.8620 ± 0.0040	1,195 ± 35
	4–9	ETH-66927	$C_{26:0}$ FA	0.8932 ± 0.0114	910 ± 105
	10–12	COL2359[a]	terr. Plant	0.9210 ± 0.0040	660 ± 40
	105–107	COL2363[a]	bulk OC	0.7790 ± 0.0040	2,005 ± 40
		COL2305[a]	carbonate	0.8769 ± 0.0048	1,055 ± 45
	103–108	COL3942[a]	$C_{16:0}$ FA	0.8820 ± 0.0180	1,005 ± 170
		ETH-66929	$C_{26:0}$ FA	0.7565 ± 0.0074	2,240 ± 80
	308–313	COL3339	bulk OC	0.6601 ± 0.0037	3,340 ± 45
		COL3944[a]	$C_{16:0}$ FA	0.7795 ± 0.0180	2,000 ± 190
		ETH-66931	$C_{26:0}$ FA	0.6916 ± 0.0060	2,960 ± 70
	468–472	COL3340	bulk OC	0.6327 ± 0.0037	3,680 ± 45
		COL3946[a]	$C_{16:0}$ FA	0.7510 ± 0.0180	2,255 ± 200
		ETH-66933	$C_{26:0}$ FA	0.6291 ± 0.0066	3,725 ± 85
	612–617	COL3341	bulk OC	0.4658 ± 0.0029	6,140 ± 50
		COL3948[a]	$C_{16:0}$ FA	0.5871 ± 0.0180	4,275 ± 240
		ETH-66935	$C_{26:0}$ FA	0.5362 ± 0.0051	5,010 ± 75
	720–725	COL3342	bulk OC	0.4571 ± 0.0030	6,290 ± 55
		COL3950[a]	$C_{16:0}$ FA	0.5397 ± 0.0180	4,955 ± 260
		ETH-66937	$C_{26:0}$ FA	0.4810 ± 0.0053	5,880 ± 90
	820–825	COL3952[a]	$C_{16:0}$ FA	0.5694 ± 0.0180	4,535 ± 250
		ETH-66939	$C_{26:0}$ FA	0.4369 ± 0.0060	6,650 ± 110
	848–850	COL2541[a]	bulk OC	0.3100 ± 0.0021	9,295 ± 55
	988–993	COL3343	bulk OC	0.2995 ± 0.0024	9,685 ± 65
		COL3954[a]	$C_{16:0}$ FA	0.3716 ± 0.0180	7,970 ± 380
		ETH-66941	$C_{26:0}$ FA	0.3391 ± 0.0054	8,690 ± 130
	992–994	COL2840[a]	terr. Plant	0.3330 ± 0.0040	8,830 ± 100
	994–996	COL2841[a]	terr. Plant	0.3280 ± 0.0040	8,970 ± 110
Rauer Group, East Antarctica					
Co1010	4–6	KIA34076[b]	bulk OC	0.8920 ± 0.0087	920 ± 80
	102–110	COL3023	bulk OC	0.7954 ± 0.0032	1,840 ± 30
		ETH-76023	$C_{16:0}$ FA	0.8345 ± 0.0073	1,445 ± 70
	542–552	COL3024	bulk OC	0.6395 ± 0.0027	3,590 ± 35
	949–959	COL3025	bulk OC	0.4889 ± 0.0023	5,750 ± 35
	1,103–1,113	COL3026	bulk OC	0.4284 ± 0.0020	6,810 ± 35
		ETH-76025	$C_{16:0}$ FA	0.4408 ± 0.0087	6,580 ± 160
	1,547–1,557	COL3027	bulk OC	0.3330 ± 0.0017	8,835 ± 40
	1729–1737	COL3028	bulk OC	0.2940 ± 0.0015	9,840 ± 40
		ETH-76024	$C_{16:0}$ FA	0.3419 ± 0.0122	8,620 ± 285
	1999–2005	COL4989	bulk OC	0.0014 ± 0.0004	>54,000

Table 1
Continued

Core	Depth (cm)	AMS lab ID	Dated material	$F^{14}C \pm 1\sigma$	^{14}C age (yr BP) $\pm 1\sigma$
		ETH-80013	$C_{14:0}$ FA	<0.0042	>43,000
		ETH-80014	$C_{22:0}$ FA	<0.0042	>43,000
		ETH-80015	$C_{24:0}$ FA	<0.0042	>43,000

Note. CRSA results were corrected for process blanks and methylation.
[a]Data previously published in Berg, White, Jicov, et al. (2019). [b]Data previously published in Berg et al. (2010).

(0.2940 ± 0.0015; 9,840 ± 40 ^{14}C yr BP) (Table 1 and Figure 3). $F^{14}C$ values of $C_{14:0}$, $C_{22:0}$, and $C_{24:0}$ FAs from 1,999 cm depth are <0.0042, that is, were not distinguishable from the background in agreement with corresponding results for bulk OC (Table 1, Figure 3).

5. Discussion

As outlined above, major difficulties in interpreting sedimentary ^{14}C ages in Antarctic coastal settings arise from contributions of petrogenic OC and from unknown and variable reservoir effects. In the Subantarctic, terrestrial organic matter derived from plants and soil in the catchment is an additional source of OC, which may affect ^{14}C ages of bulk OC in coastal settings. To explore the implications for the development of age-depth models, we compare three different settings to i) identify general effects of petrogenic OC on ^{14}C ages in Antarctic marine environments, ii) discuss evidence for the extent of marine reservoir effects in different regions, and iii) to test if marine and (in case of the Subantarctic) terrestrial biogenic compounds in coastal marine sediments can provide reliable ^{14}C ages for dating sediments in the Antarctic and Subantarctic.

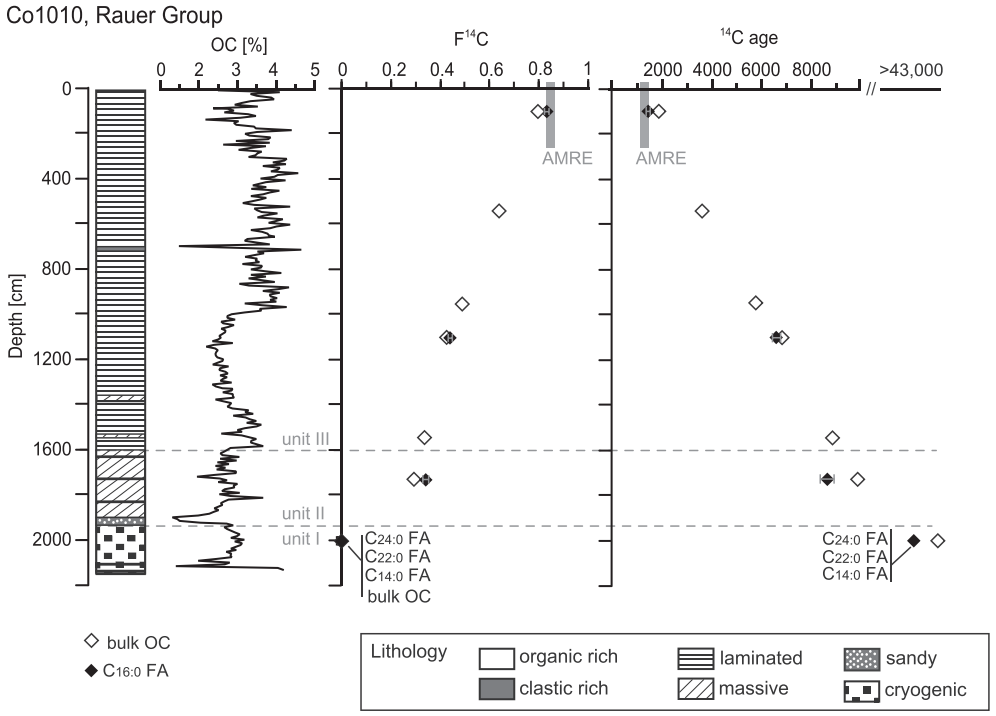

Figure 3. Core Co1010: Lithology, total organic carbon (OC) (wt%), $F^{14}C$ and corresponding ^{14}C ages bulk OC and $C_{16:0}$ FA (error bars represent 1σ uncertainty ranges, error bars for bulk OC $F^{14}C$ values are well within size of symbols). For sediment depth 1999 cm $C_{14:0}$, $C_{22:0}$ and $C_{24:0}$ FA were isolated. $C_{16:0}$ FA was lost during sample preparation. AMRE = Antarctic marine reservoir effect 1,100–1,300 years.

5.1. Influence of Petrogenic and Reworked OC on Bulk ^{14}C Ages in the (Sub-)Antarctic

Bulk sedimentary OC represents an admixture of OC from various sources (petrogenic, marine and terrestrial), thus resulting in $F^{14}C$ values, which do not necessarily reflect the actual age of sedimentation. In Cumberland West Bay, South Georgia (core PS81/283-1), $F^{14}C$ values of bulk OC relative to co-occurring FA (HMW and LMW) and carbonates correspond to age offsets of > 8,000 years in all three investigated samples (Figure 2a). The low bulk OC $F^{14}C$ values are indicative for high proportions of ^{14}C-free petrogenic OC ($F^{14}C = 0$) and/or other sources of ^{14}C-depleted OC in the bulk sedimentary OC pool. To estimate the petrogenic OC contribution to the surface sediments, we use mass balance to determine the respective fractional abundances of marine, terrestrial and petrogenic OC. We define the $F^{14}C$ value of marine OC using both the $C_{16:0}$ FA and foraminifer $F^{14}C$ values in the core top sample of PS81/283-1 and include the uncertainty from using both values (plus respective errors) in our results. The terrestrial $F^{14}C$ value is best represented by the $C_{26:0}$ FA in the core top sample of Co1305. Since the $F^{14}C$ value of $C_{26:0}$ FA is bracketed by the $C_{16:0}$ FA and foraminifer $F^{14}C$ values, we can use a combined marine+terrestrial endmember to estimate the contribution of petrogenic OC:

$$F^{14}C_{(\text{bulk OC})} = f_{(\text{petrogenic})} \times F^{14}C_{(\text{petrogenic})} + f_{(\text{marine + terrestrial})} \times F^{14}C_{(\text{marine + terrestrial})}$$

where $F^{14}C_{(\text{bulk OC})}$, $F^{14}C_{(\text{petrogenic})}$, and $F^{14}C_{(\text{marine+terrestrial})}$ represent the ^{14}C isotopic composition of the measured bulk OC, petrogenic OC, and marine + terrestrial OC, and $f_{(\text{petrogenic})}$ and $f_{(\text{marine+terrestrial})}$ represent their respective fractional abundances with $f_{(\text{petrogenic})} + f_{(\text{marine+terrestrial})} = 1$.

Accordingly, the $F^{14}C$ value of OC in surface sediments at site PS81/283-1 can be explained by a petrogenic OC contribution of 75–78%. Considerable contributions of petrogenic OC likely also control the bulk OC ^{14}C ages downcore: The apparent age reversal of bulk OC at 211 cm core depth likely reflects a lower contribution of petrogenic OC (65–68%). The finding of petrogenic OC being the dominant OC carbon fraction in core PS81/283-1 is not well reflected in C/N ratios of 8.3 ± 0.3, since petrogenic OM is generally characterized by much higher C/N ratios (low N contents) (e.g., Schneider-Mor et al., 2012). In this specific case, the C/N ratio alone is not indicative for the source of OC in the sediment, due to the complex mixture of various sedimentary organic compounds. The $F^{14}C$ values of bulk OC and FAs therefore can be used to assess the petrogenic contribution in marine sediments, given that the main OC sources are well represented by two endmembers (petrogenic and marine + terrestrial). This may not be the case in settings with e.g., high contributions from terrestrial sources with a more depleted ^{14}C isotopic composition (see also discussion in section 5.4). In Cumberland West Bay, petrogenic OC likely originates from erosion of bedrock (Mesozoic gray wacke and pelites; Clayton, 1982a, 1982b). Other ^{14}C-depleted OC sources may include marine and terrestrial deposits such as paleosols and/or marine sediments in the catchment of the fjord. The main input pathway of ancient OC likely is erosion and re-working by the glaciers terminating to the southeast of the coring location (Figure 1). In Antarctica, high bulk OC ^{14}C ages were reported from shelf sediments deposited in front of ice shelf calving fronts, for example, around the Antarctic Peninsula (e.g., Rosenheim et al., 2008, 2013; Subt et al., 2017) and in the Ross Sea (e.g., Andrews et al., 1999; Ohkouchi et al., 2003), reflecting relatively high and variable petrogenic OC contributions in surface sediments. In the Ross Sea the high spatial variation of petrogenic OC (ranging from 13% to 90%) is mainly controlled by the proximity to the Ross Ice Shelf and the lithology of the catchments (e.g., coal bearing strata in the catchment; Ohkouchi & Eglinton, 2006). Around the Antarctic Peninsula, highest ^{14}C ages and correspondingly high contributions of petrogenic OC occur proximal to ice shelf fronts (Rosenheim et al., 2013; Subt et al., 2017). The proximity to the source of petrogenic OC input is one factor influencing ^{14}C ages. Other site-specific factors likely play a role in each case, for example, hydrodynamic sorting and differential deposition of particles as has been shown for shelf settings (e.g., Mollenhauer & Eglinton, 2007). Analogous to our sediment record from the Subantarctic fjord, $F^{14}C$ values of LMW FAs extracted from sediments in the Ross Sea are less depleted in ^{14}C than the bulk OC (Ohkouchi et al., 2003; Yokoyama et al., 2016). This indicates that the LMW FA are less affected by petrogenic contributions than the bulk of sedimentary OC although they may be preserved over geological time scales (Kvenvolden, 1966).

In contrast to the highly siliciclastic sediments in Cumberland West Bay, the more biogenic sediments from the marine inlets in South Georgia (Co1305) and East Antarctica (Co1010) contain low proportions of

petrogenic OC (0–5%) as based on above mass balance. In Rauer Group (core Co1010), very low petrogenic OC contribution likely results from a lack of OC in the Proterozoic granulites in the catchment (Harley, 1988) and/or low clastic input from land and the adjacent ice sheet margin. In contrast, the inlet in South Georgia receives allochthonous OC as suspended and ice rafted material from Cumberland West Bay and from the surrounding catchment (Berg, White, Jivcov, et al., 2019). However, $F^{14}C$ values of surface sediments indicate that the contribution of the petrogenic component is relatively low (4–5%) compared to the adjacent fjord. In both investigated marine inlets, a relatively high OC input from autochthonous production and, in case of South Georgia, additional input from contemporaneous terrestrial OC likely dilutes potential petrogenic OC inputs.

The $F^{14}C$ values of LMW FA in the fjord sediments of Cumberland West Bay (PS81/283-1) indicate that these compounds can provide an improved age constraint. This finding is particularly relevant for sites that are strongly affected by high siliciclastic input from glaciers or ice shelves such as in fjords and on the Antarctic shelves (e.g., Ohkouchi et al., 2003; Yokoyama et al., 2016). In these settings, CSRA also provides a means of quantifying the input of petrogenic OC assuming that samples do not contain re-worked ancient LMW FA.

5.2. Influence of Reservoir Effects on Marine ^{14}C Ages in the (Sub-)Antarctic

^{14}C ages derived from marine materials need to be corrected for the marine reservoir effect when used for age determination. The mean Antarctic marine reservoir effect (AMRE) ranges from 1,100 to 1,300 years (e.g., Berkman & Forman, 1996). Deviations of Antarctic core top sediment ages from the AMRE value are often attributed to a local effect, which is then used to correct downcore sediment ages (e.g., Andrews et al., 1999; Hemer & Harris, 2003; Hillenbrand et al., 2009). As shown for the sediment record from Cumberland West Bay, bulk OC analysis does not allow distinguishing between the reservoir age of autochthonous OC and contributions of petrogenic OC. Therefore, this approach may lead to large age offsets from the actual AMRE, especially in settings where petrogenic input is high and variable over time. As site-specific DIC $F^{14}C$ values can be reflected in LMW FA from surface sediments (Ohkouchi et al., 2003), we will discuss to what extent CRSA can be indicative for marine reservoir effects.

In the marine inlet in Rauer Group (core Co1010) no compound-specific ^{14}C age could be obtained for the uppermost part, due to insufficient sample material. The $F^{14}C$ value of bulk OC in the uppermost analyzed sample (4–6 cm depth) is 0.8920 ± 0.0087, corresponding to 920 ^{14}C years BP. As discussed above, the petrogenic OC input to the marine inlet is low, thus, bulk OC ^{14}C ages likely reflect the local reservoir effect, which is lower than the mean AMRE in this specific setting, The $F^{14}C$ value of the $C_{16:0}$ FA at 102 cm depth is close to modern AMRE supporting a consistently lower than AMRE reservoir age at this site. Surface sediment bulk OC ^{14}C ages from two other marine inlets in Rauer Group are lower than the mean AMRE as well (Berg et al., 2013) supporting a modern reservoir age of c. 920 years for the marine inlets in Rauer Group. Lower $F^{14}C_{DIC}$ values compared to AMRE likely result from modified water masses in the coastal and shelf areas of Prydz Bay (Borchers et al., 2016; Smith et al., 1984) that are also reflected in $F^{14}C$ values of feathers and bones of modern sea birds (corresponding to 710 to 895 years; Berg, White, Hermichen, et al., 2019).

In order to identify reservoir effects, carbonate fossils such as foraminifers (planktic and benthic) and other calcifying organisms are typically used (e.g., Graham et al., 2017). Since core PS81/283-1 from Cumberland West Bay contains some carbonaceous remains, we compare our CSRA results with carbonate ^{14}C ages of the same samples. ^{14}C ages of benthic foraminifers from the uppermost sample (1–2 cm) of core PS81/283-1 ($1,070 \pm 60$ and $1,080 \pm 50$ ^{14}C yr BP) are in accordance with a marine reservoir age of c. 1,100 ^{14}C yr BP determined for upper circumpolar deep water (CDW), the subsurface water mass in Cumberland Bay (Geprägs et al., 2016; Graham et al., 2017). ^{14}C ages of $C_{16:0 + 18:0}$ FA isolated from the same sample (PS81/283-1, 1–2 cm) are younger than those of the benthic foraminifers (corresponding to 300–570 years). This pattern is also evident in the sample from 211 cm core depth, where we find a 1,160–1,570 years off-set between LMW FA and carbonate (mollusk shell debris). For Cumberland West Bay a source of ^{14}C-depleted carbon could be from methane, which could potentially alter ^{14}C ages of carbonate fossils by the formation of secondary carbonates with depleted ^{14}C isotopic composition. However, $F^{14}C$ values from leached outer and inner layers of the dated mollusk debris do not show systematic offsets (Table S3) indicating that secondary calcification is either negligible or $F^{14}C$ values of secondary

carbonates do not differ from DIC $F^{14}C$ values. Different $F^{14}C$ values for carbonates and LMW FA could be explained by different water masses as habitats of the ^{14}C–dated calcifying organisms and phytoplankton (main source of LMW FA), which could be a function of water depth. Alternatively, the age offset could also depend on variable conditions in the fjord like intensity of meltwater inflow, thickness of freshwater layer, and stability of stratification of the water column. In addition to effects attributable to the respective carbon pools, sedimentation-related processes like winnowing or reworking of the carbonates may affect age offsets between the different analyzed materials. For future studies comparison of concurrent LMW FA and carbonate ages in different depth intervals could be used to explore variable aquatic reservoir effects. However, to accurately quantify the magnitude of reservoir age variability, independent stratigraphic markers such as tephra layers and/or fallout radionuclides in near-surface sediments would be necessary.

5.3. ^{14}C Isotopic Signatures of Terrestrial OC in Subantarctic Marine Sediments

In contrast to the Antarctic, near shore marine sediments in South Georgia may receive considerable inputs of terrestrial OC from the surrounding vegetated catchment. In lake sediment studies, terrestrial plant remains are typically the primary targets for ^{14}C-based age determination (e.g., Strother et al., 2014; van der Bilt et al., 2017), since land plants are generally not affected by reservoir effects and thus may provide contemporaneous ^{14}C ages. In this section, we discuss if ^{14}C ages of HMW FA that mainly derive from terrestrial higher plants may also be used for establishing valid age-depth models for near shore marine records.

In both investigated records from South Georgia, the occurrence of HMW FA reflects terrestrial OM in the marine sediments, although we acknowledge that FA only represent a small fraction of the terrestrial OM continuum. In Cumberland West Bay (core PS81/283-1) the ^{14}C ages of plant wax compounds and of LMW FA agree within analytical uncertainty in the sample from 211 cm depth and are slightly older than LMW FA in the lower sample from 451 cm depth (Figure 2b and Table 1). In core Co1305, ^{14}C ages of HMW FA are older than the LMW FA from the same sample, except for the lowermost depth, where HMW and LMW FA agree within analytical uncertainty (Figure 2b and Table 1). This suggests that the terrestrial FA in the marine sediments contains some proportion of FA that did not form at the time of sediment deposition, but were stored in soils or peat deposits for hundreds of years before they were transported to the marine inlet.

The pattern of ^{14}C-depletion of terrestrial biomarkers relative to the depositional age of the sediment that we find in marine sediments in South Georgia is consistent with evidence from marine sites from the Arctic (e.g., Drenzek et al., 2007; Vonk et al., 2014) as well as from non-polar regions (e.g., Kusch et al., 2010; Schefuß et al., 2016). In the Arctic, plant-wax derived FA in marine surface sediments on the shelf provided ^{14}C ages of up to several thousand years (e.g., 5.5 to 18 kyr on the East Siberian Shelf, Vonk et al., 2014). In this specific environment, terrestrial OM is delivered by large river systems and active coastal erosion releasing OC locked in permafrost for millennia (e.g., Vonk et al., 2014; Winterfeld et al., 2018). As opposed to the Arctic, where terrestrial deposits range back to the Pleistocene, the comparably younger ^{14}C ages of plant-wax derived FA in marine sediments in South Georgia indicate a largely Holocene age of the terrestrial OM. In the temperate Fiordland, New Zealand, biomarker and bulk OC ages show that the majority of terrestrial OM in fjord sediments is modern (Cui et al., 2017). In contrast to the temperate region with a pronounced morphological relief, less dense vegetation cover and peat formation glacially flattened or excavated morphology in the Subantarctic may result in higher proportions of reworked, older terrestrial OM in the coastal marine environment. This makes HMW FA ^{14}C ages less suitable for determining the actual sediment age than LMW FA in the Subantarctic. Instead, the variable age differences between the terrestrial HMW and predominantly marine LMW biomarkers downcore may provide information on past environmental changes (Figure 4). $F^{14}C$ values of HMW FA from core Co1305 suggest a predominantly Holocene age of the terrestrial OC in the coastal marine environment, which is consistent with the deglaciation history of South Georgia. The island was covered by an ice cap prior to c. 16 kyr before present (Barlow et al., 2016; White et al., 2018) and most terrestrial OM pre-dating glaciation may have been lost by glacial erosion. A relatively low $F^{14}C$ offset between LMW and HMW fatty acids in the early Holocene part of Co1305 (Figure 4) indicates a relatively high input of contemporaneous plant material, which is consistent with the widespread onset of peat formation and expansion of terrestrial vegetation on South Georgia during that time (Berg, White, Jivcov, et al., 2019; Van der Putten & Verbruggen, 2005). In contrast, a ^{14}C maximum

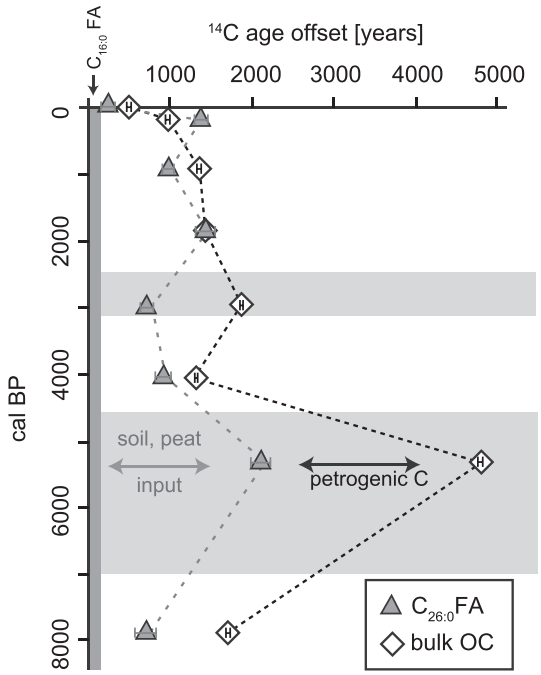

Figure 4. Age off-set of bulk OC and $C_{26:0}$ FA relative to $C_{16:0}$ FA for core Co1305 shown versus age. The age-depth model was previously presented and discussed in Berg, White, Jivcov, et al. (2019). Gray horizontal bars indicate periods of advanced cirque glaciers in the catchment and increased deposition of ice rafted debris in the inlet (Berg, White, Jivcov, et al., 2019; Oppedal et al., 2018).

offset between LMW and HMW FA was found for the period of advanced cirque glaciers in the catchment of the inlet between 7,200 and 4,800 yr BP (Oppedal et al., 2018) (Figure 4). This indicates that increased erosion and run-off likely resulted in reworking of plant-derived material that was previously fixed in soils and peat deposits. Higher erosion and associated input of petrogenic OC is also evidenced by the age offset between LMW and HMW FA relative to bulk OC (Figure 4).

5.4. Implications for Age-Depth Models

In order to illustrate the implications of our findings for core chronologies, we developed comparative age-depth models based on ^{14}C ages of each of the analyzed materials (bulk OC, carbonates, LMW FA and HMW FA; Figure 5). For materials of marine origin (carbonates, LMW FA) we use a constant marine reservoir age for each downcore record, that is, 920 years (ΔR = 558) for core Co1010 (Rauer Group) based on the bulk OC core top $F^{14}C$ value (Table 1). For the site in Cumberland West Bay (South Georgia; core PS81/283-1), $F^{14}C$ values for carbonates and $C_{16:0}$ FA are different and we therefore provide individual reservoir corrections for carbonates (1,070 years based on benthic foraminifers, ΔR = 670) and LMW FA (645 years, core top value; ΔR = 245). In the absence of a surface $F^{14}C$ value for $C_{16:0}$ FA in core Co1305, we use the same reservoir correction used for PS81/283-1, since water exchange between the inlet and the fjord likely results in similar reservoir ages. For cores Co1305 and Co1010, we also show age-depth models based on bulk OC ^{14}C ages, each reservoir-corrected using the surface sediment bulk OC $F^{14}C$ value (Co1305, ΔR = 793) (Figures 5b and 5c). For core PS81/283-1, OC ages were not considered for the age-depth model, since high petrogenic contribution impedes a reasonable age interpretation.

Least ambiguity between the different age-depth models is evident for the record from Rauer Group (Figure 5c). For core Co1010, age-depth models based on OC and $C_{16:0}$ FA mostly overlap within their respective 95% confidence intervals (Figure 5c). This illustrates that LMW FA as well as bulk OC ^{14}C ages can provide valid age information when input of petrogenic carbon is low. Although the age-depth model based on $C_{16:0}$ FA provides wider age ranges than the model based on OC (due to the larger analytical uncertainty for the smaller samples), analysis of both materials can be desirable to assess biases from petrogenic OC. In diatom oozes recovered in core U1357A from the continental shelf off Wilkes Land, East Antarctica (Figure 1), bulk OC ^{14}C ages become successively older with depth (Yamane et al., 2014). CSRA of $C_{16:0}$ and $C_{16:1}$ FA from this core provide a consistent age-depth relationship as well, but moreover reveal changes in sedimentation rate and input of petrogenic material, which was not evident from bulk ^{14}C ages alone (Yamane et al., 2014; Figure 5d).

In core PS81/283-1 (Cumberland West Bay), all age-depth models conform in a late Holocene age of the record, which is a much improved age estimate compared to bulk OC ^{14}C-ages (Figure 5a).

In core PS81/283-1, age-depth models based on carbonates and LMW FA differ. The LMW FA based age model provides younger ages and variable sedimentation rates (Figure 5a). This difference likely results from the respective reservoir corrections included in the models, which may be applicable for the surface samples but not necessarily for the downcore correction. The relatively large analytical uncertainties of some of the $F^{14}C$ values result in large probability distributions during calibration to obtain an age-depth model. This effect is particularly evident for core PS81/283-1 (211 cm core depth, Figure 5a). In contrast to the small offset between $F^{14}C$ values of HMW FA and LMW FA, the respective age-depth models do not overlap and produce significantly higher ages for the terrestrial derived OC fraction, which is an effect of the different calibration datasets used for marine and terrestrial OC (Figure 5a). In this specific environmental setting where OM content is low and input of petrogenic OC is high, LMW FA ^{14}C ages can be useful to obtain information on sediment age. This adds to previous results by Yokoyama et al. (2016), who showed that LMW FA

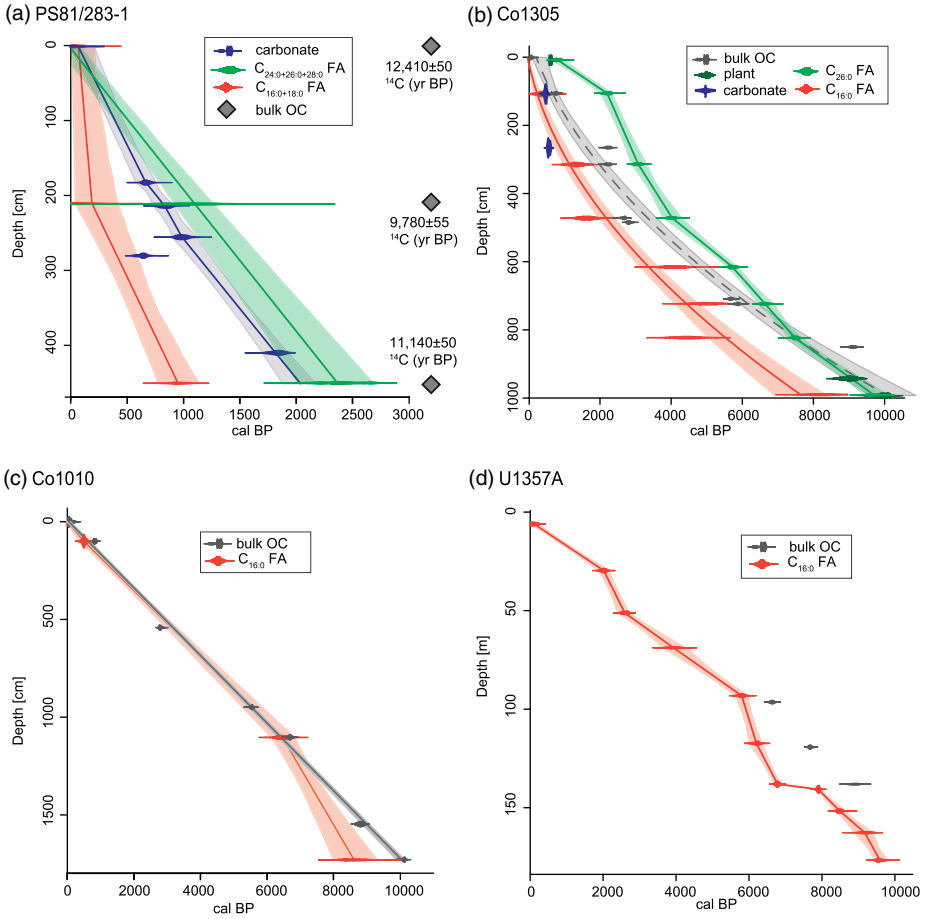

Figure 5. (a) to (c) Age depth-models for cores PS81/283-1, Co1305, Co1010 based on the $F^{14}C$ values of the different OC fractions. Reservoir corrections and calibration are described in section 5.4. Carbonate and plant ^{14}C ages shown for core Co1305 have previously been published by Berg, White, Jivcov, et al. (2019). Conventional ^{14}C ages are given in Table 1. (d) Age-depth model for core U1357A is based on CSRA and bulk OC ages published by Yamane et al. (2014).

^{14}C ages in Ross Sea sediments are less influenced by petrogenic carbon and CSRA provides improved age assignment relative to bulk OC analysis. However, the age-depth models for core PS81/283-1 and Co1305 also illustrate that reservoir corrections may be complicated for the LMW FA, since the $F^{14}C$ value represents an integrated phytoplankton signal. In core Co1305, age-depth models based on HMW and LMW FA have a mean offset of 2,160 years (Figure 5b). This shows that the source of the material used for ^{14}C analysis has a significant impact on the resulting age-depth model in this coastal marine setting. More specifically, ^{14}C analysis of land plant derived material may lead to an age overestimation of the actual sediment age, while LMW FA are affected by complex aquatic reservoir effects.

6. Conclusion

We present a comprehensive CSRA data set for Subantarctic South Georgia and used this to assess the efficacy of this method as a tool to improve sediment chronologies. In the three investigated marine records, LMW FA including $C_{16:0}$ and $C_{18:0}$ were the least ^{14}C-depleted compounds. These compounds mainly originate from phytoplankton and thus represent autochthonous OC produced syndepositionally. Thus, CSRA of these biomarkers can improve sediment chronologies when petrogenic input is high and carbonaceous fossils are rare/absent such as in Antarctic and Subantarctic shelf and fjord settings. This analytical tool is most helpful at sites that have contact with the open ocean, hence where co-sedimentation of contemporary marine OC occurs. Analogous to bulk OC analysis, CSRA may not improve sediment chronologies in settings

where deposition of fresh OM is restricted (e.g. by site-specific water circulation patterns in sub-ice shelf settings). In low OC sediments with high petrogenic input, CSRA may be the only means of obtaining meaningful age information. However, it should be assured that sufficient amounts of isolated compounds (>20 μg carbon) can be obtained from the sediments to achieve high precision ages in particular if sedimentary OC is old. In settings where petrogenic input is low and the proportions of autochthonous marine OC is high (such as the marine inlet of Rauer Group), bulk OC likely provides good age control. In contrast, bulk OC ^{14}C ages do not accurately reflect sedimentation ages in marine inlets in the Subantarctic, where terrestrial OC is an additional OC source that may affect bulk OC ^{14}C ages. Supplementing high-resolution bulk OC records with lower resolution CSRA records will aid at assessing changes in petrogenic (and terrestrial) input and improving age estimates of marine sediment records.

Conflict of Interest

The authors declare no conflicts of interest.

Data Availability Statement

Data presented in Table 1 and supporting information are available via PANGAEA geoscientific database (https://doi.org/10.1594/PANGAEA.920081).

Acknowledgments

This work was supported by the Deutsche Forschungsgemeinschaft (DFG) in the framework of the priority program "SPP1158 Antarctic Research with comparative investigations in Arctic ice areas" by Grants BE 4764/1-1 and BE 4764/3-1. RV Polarstern expedition PS81 and G. K. were supported by the Alfred-Wegener-Institute, Helmholtz Centre PACES II (Polar Regions and Coasts in the changing Earth System) program. Additional funding was provided to S. B. by a University of Cologne (UoC) Postdoc grant. Open access funding enabled and organized by Projekt DEAL.

References

Andrews, J. T., Domack, E. W., Cunningham, W. L., Leventer, A., Licht, K. J., Jull, A. J. T., et al. (1999). Problems and possible solutions concerning radiocarbon dating of surface marine sediments, Ross Sea, Antarctica. *Quaternary Research*, *52*, 206–216.

Bard, E., Tuna, T., Fagault, Y., Bonvalot, L., Wacker, L., Fahrni, S., & Synal, H.-A. (2015). AixMICADAS, the accelerator mass spectrometer dedicated to ^{14}C recently installed in Aix-En-Provence, France. *Nuclear Instruments and Methods in Physics Research Section B: Beam Interaction with Material and Atoms*, *361*, 80–86.

Barlow, N. L. M., Bentley, M. J., Spada, G., Evans, D. J. A., Hansom, J. D., Brader, M. D., et al. (2016). Testing models of ice cap extent, South Georgia, sub-Antarctic. *Quaternary Science Reviews*, *154*, 157–168. https://doi.org/10.1016/j.quascirev.2016.11.007

Berg, S., Leng, M. J., Kendrick, C. P., Cremer, H., & Wagner, B. (2013). Bulk sediment and diatom silica carbon isotope composition from coastal marine sediments off East Antarctica. *SILICON*, *5*(1), 19–34. https://doi.org/10.1007/s12633-012-9113-3

Berg, S., Melles, M., Gore, D. B., Verkulich, S., & Pushina, Z. (2020). Postglacial evolution of marine and lacustrine water bodies in Bunger Hills. *Antarctic Science*, *32*(2), 107–129. https://doi.org/10.1017/S0954102019000476

Berg, S., Wagner, B., Cremer, H., Leng, M. J., & Melles, M. (2010). Late Quaternary environmental and climate history of Rauer group, East Antarctica. *Palaeogeography, Palaeoclimatology, Palaeoecology*, *297*(1), 201–213. https://doi.org/10.1016/j.palaeo.2010.08.002

Berg, S., White, D., Hermichen, W.-D., & Emmerson, L. (2019). Late Holocene colonization of snow petrels (*Pagodroma nivea*) of the Prince Charles mountains, Antarctica. *Polar Biology*, *42*(6), 1167–1173. https://doi.org/10.1007/s00300-019-02509-0

Berg, S., White, D. A., Jivcov, S., Melles, M., Leng, M. J., Rethemeyer, J., et al. (2019). Holocene glacier fluctuations and environmental changes in sub-Antarctic South Georgia. *Quaternary Research*, *91*(1), 132–148. https://doi.org/10.1017/qua.2018.85

Berkman, P., & Forman, S. (1996). Pre-bomb radiocarbon and the reservoir correction for calcareous marine species in the Southern Ocean. *Geophysical Research Letters*, *23*, 363–366.

Blaauw, M. (2010). Methods and code for 'classical' age-modelling of radiocarbon sequences. *Quaternary Geochronology*, *5*, 512–518.

Bohrmann, G. (Ed.). (2013). The expedition of the research vessel "Polarstern" to the Antarctic in 2013 (ANT-XXIX/4). Reports on Polar and Marine Research 668, 117–135.

Borchers, A., Dietze, E., Kuhn, G., Esper, O., Voigt, I., Hartmann, K., & Diekmann, B. (2016). Holocene ice dynamics and bottom-water formation associated with cape Darnley polynya activity recorded in Burton Basin, East Antarctica. *Marine Geophysical Research*, *37*(1), 49–70. https://doi.org/10.1007/s11001-015-9254-z

Clayton, R. A. S. (1982a). The geology of North-Western South Georgia: III. Petrology of the Cumberland Bay formation. *British Antarctic Survey Bulletin*, *51*, 79–88.

Clayton, R. A. S. (1982b). A preliminary investigation of geochemistry of greywackes from South Georgia. *British Antarctic Survey Bulletin*, *51*, 89–109.

Cremer, H., Gore, D., Melles, M., & Roberts, D. (2003). Palaeoclimatic significance of late Quaternary diatom assemblages from southern Windmill Islands, East Antarctica. *Palaeogeography, Palaeoclimatology, Palaeoecology*, *195*(3-4), 261–280. https://doi.org/10.1016/S0031-0182(03)00361-4

Cui, X., Bianchi, T. S., & Savage, C. (2017). Erosion of modern terrestrial organic matter as a major component of sediments in fjords. *Geophysical Research Letters*, *44*, 1457–1465. https://doi.org/10.1002/2016GL072260

Dejardin, R., Kender, S., Allen, C. S., Leng, M. J., Swann, G. E., & Peck, V. (2018). Live (stained) benthic foraminiferal living depths, stable isotopes and taxonomy offshore South Georgia, Southern Ocean: implications for calcification depths. *Journal of Micropalentology*, *37*, 25–71. https://doi.org/10.5194/jm-0-1-2017

Drenzek, N., Montlucon, D. B., Yunker, M. B., Macdonald, R. W., & Eglinton, T. I. (2007). Constraints on the origin of sedimentary organic carbon in the Beaufort Sea from coupled molecular 13C and 14C measurements. *Marine Chemistry*, *103*(1–2), 146–162. https://doi.org/10.1016/j.marchem.2006.06.017

Eglinton, T. I., Aluwihare, L. I., Bauer, J. E., Druffel, E. R. M., & McNichol, A. P. (1996). Gas chromatographic isolation of individual compounds from complex matrices for radiocarbon dating. *Analytical Chemistry*, *68*(5), 904–912. https://doi.org/10.1021/ac9508513

Geprägs, P., Torres, M. E., Mau, S., Kasten, S., Römer, M., & Bohrmann, G. (2016). Carbon cycling fed by methane seepage at the shallow Cumberland Bay, South Georgia, sub-Antarctic. *Geochemistry, Geophysics, Geosystems*, *17*, 1401–1418. https://doi.org/10.1002/2016GC6276

Gordon, J. E., & Harkness, D. D. (1992). Magnitude and geographic variation of the radiocarbon content in Antarctic marine life: Implications for reservoir corrections in radiocarbon dating. *Quaternary Science Reviews*, *11*(7–8), 697–708. https://doi.org/10.1016/0277-3791(92)90078-M

Graham, A. G. C., Kuhn, G., Meisel, O., Hillenbrand, C. D., Hodgson, D. A., Ehrmann, W., et al. (2017). Major advance of South Georgia glaciers during the Antarctic cold reversal following extensive sub-Antarctic glaciation. *Nature Communications*, *8*(1), 14798. https://doi.org/10.1038/ncomms14798

Hall, B., Henderson, G. M., Baroni, C., & Kellogg, T. B. (2010). Constant Holocene Southern-Ocean ^{14}C reservoir ages and ice-shelf flow rates. *Earth and Planetary Science Letters*, *296*(1–2), 115–123. https://doi.org/10.1016/j.epsl.2010.04.054

Harley, S. L. (1988). Proterozoic granulites from the Rauer group, East Antarctica. I. Decompressional pressure–temperature paths deduced from mafic and felsic gneisses. *Journal of Petrology*, *29*, 1059–1095.

Hemer, M. A., & Harris, P. T. (2003). Sediment core from beneath the Amery ice shelf, East Antarctica suggest mid-Holocene ice-shelf retreat. *Geology*, *31*(2), 127–130. https://doi.org/10.1130/0091-7613(2003)031<0127:SCFBTA>2.0.CO;2

Hendy, C. H., & Hall, B. L. (2006). The radiocarbon reservoir effect in proglacial lakes: Examples from Antarctica. *Earth and Planetary Science Letters*, *241*(3–4), 413–421. https://doi.org/10.1016/j.epsl.2005.11.045

Hillenbrand, C.-D., Smith, J. A., Kuhn, G., Esper, O., Gersonde, R., Larter, R. D., et al. (2009). Age assignment of a diatomaceous ooze deposited in the western Amundsen Sea embayment after the last glacial maximum. *Journal of Quaternary Science*, *25*, 280–295.

Hodgson, D. A., Whitehouse, P. L., de Cort, G., Berg, S., Verleyen, E., Tavernier, I., et al. (2016). Rapid early Holocene sea-level rise in Prydz Bay, East Antarctica. *Global and Planetary Change*, *139*, 128–140. https://doi.org/10.1016/j.gloplacha.2015.12.020

Hogg, A. G., Hua, Q., Blackwell, P. G., Niu, M., Buck, C. E., Guilderson, T. P., et al. (2013). Shcal13 southern hemisphere calibration, 0–50,000 years cal BP. *Radiocarbon*, *55*(4), 1889–1903. https://doi.org/10.2458/azu_js_rc.55.16783

Ingalls, A. E., & Pearson, A. (2005). Ten years of compound-specific radiocarbon analysis. *Oceanography*, *18*, 18–31. https://doi.org/10.5670/oceanog.2005.22

Kusch, S., Rethemeyer, J., Schefuß, E., & Mollenhauer, G. (2010). Controls on the age of vascular plant biomarkers in Black Sea sediments. *Geochimica et Cosmochimica Acta*, *74*, 7031–7047.

Kvenvolden, K. A. (1966). Molecular distributions of normal fatty acids and paraffins in some lower cretaceous sediments. *Nature*, *209*(5023), 573–577. https://doi.org/10.1038/209573a0

Majevski, W. (2005). Benthic foraminiferal communities: Distribution and ecology in Admiralty Bay, King George Island, West Antarctica. *Polish Polar Research*, *26*, 159–214.

Mollenhauer, G., & Eglinton, T. (2007). Diagenetic and sedimentological controls on the composition of organic matter preserved in California Borderland Basin sediments. *Limnology and Oceangraphy*, *52*, 558–576.

Moreton, S. G., Rosqvist, G. C., Davies, S. J., & Bentley, M. J. (2004). Radiocarbon reservoir ages from freshwater lakes, South Georgia, sub-Antarctic: Modern analogues from particulate organic matter and surface sediments. *Radiocarbon*, *46*(2), 621–626. https://doi.org/10.1017/S0033822200035669

Ohkouchi, N., & Eglinton, T. (2006). Radiocarbon constraint on relict organic carbon contributions to Ross Sea sediments. *Geochemistry, Geophysics, Geosystems*, *7*, Q04012. https://doi.org/10.1029/2005GC001097

Ohkouchi, N., Eglinton, T., & Hayes, J. (2003). Radiocarbon dating of individual fatty acids as a tool for refining Antarctic margin sediment chronologies. *Radiocarbon*, *45*(1), 17–24. https://doi.org/10.1017/S0033822200032355

Ohkouchi, N., & Eglinton, T. J. (2008). Compound specific radiocarbon dating of Ross Sea sediments: A prospect for constructing chronologies in high-latitude oceanic sediments. *Quaternary Geochronology*, *3*(3), 235–243. https://doi.org/10.1016/j.quageo.2007.11.001

Oppedal, L. T., Bakke, J., Paasche, Ø., Werner, J. P., & van der Bilt, W. G. M. (2018). Cirque glaciers on South Georgia shows centennial variability over the last 7000 years. *Frontiers in Earth Science*, *6*. https://doi.org/10.3389/feart.2018.00002

Reimer, P. J., Bard, E., Bayliss, A., Beck, J. W., Blackwell, P. G., Ramsey, C. B., et al. (2013). INTCAL13 and Marine13 radiocarbon age calibration curves 0–50,000 years cal BP. *Radiocarbon*, *55*(4), 1869–1887. https://doi.org/10.2458/azu_js_rc.55.16947

Reimer, P. J., Brown, T. A., & Reimer, R. W. (2004). Discussion: Reporting and calibration of post-bomb ^{14}C data. *Radiocarbon*, *46*, 1299–1304.

Rethemeyer, J., Gierga, M., Heinze, S., Stolz, A., Wotte, A., Wischhöfer, P., et al. (2019). Current sample preparation and analytical capabilities of the radiocarbon laboratory at Cologne AMS. *Radiocarbon*, *61*(5), 1449–1460. https://doi.org/10.1017/RDC.2019.16

Römer, M., Torres, M., Kasten, S., Kuhn, G., Graham, A. G. C., Mau, S., et al. (2014). First evidence of widespread active methane seepage in the Southern Ocean, off the sub-Antarctic island South Georgia. *Earth and Planetary Science Letters*, *403*, 166–177. https://doi.org/10.1016/j.epsl.2014.06.036

Rosenheim, B., Day, M. B., Domack, E., Schrum, H., Benthien, A., & Hayes, J. M. (2008). Antarctic sediment chronology by programmed-temperature pyrolysis: Methodology and data treatment. *Geochemistry, Geophysics, Geosystems*, *9*, Q04005. https://doi.org/10.1029/2007GC001816

Rosenheim, B. E., Santoro, J. A., Gunter, M., & Domack, E. W. (2013). Antarctic sediment 14C dating using ramped pyrolysis: An example from the Hugo Island trough. *Radiocarbon*, *55*(1), 115–126. https://doi.org/10.2458/azu_js_rc.v55i1.16234

Schefuß, E., Eglinton, T. I., Spencer-Jones, C. L., Rullkötter, J., de Pol-Holz, R., Talbot, H. M., et al. (2016). Hydrologic control of carbon cycling and ages carbon discharge in the Congo River basin. *Nature Geoscience*, *9*(9), 687–690. https://doi.org/10.1038/ngeo2778

Schneider-Mor, A., Alsenz, H., Ashckenazi-Polivoda, S., Illner, P., Abramovich, S., Feinstein, S., et al. (2012). Paleoceanographic reconstruction of the late cretaceous oil shale of the Negev, Israel: Integration of geochemical, and stable isotope records of the organic matter. *Palaeogeography, Palaeoclimatology, Palaeoecology*, *319–320*, 46–57.

Smith, N. R., Zhaoqian, D., Kerry, K. R., & Wright, S. (1984). Water masses and circulation in the region of Prydz Bay, Antarctica. *Deep-Sea Research*, *31*(9), 1121–1147. https://doi.org/10.1016/0198-0149(84)90016-5

Strother, S. L., Salzmann, U., Roberts, S. J., Hodgson, D. A., Woodward, J., Van Nieuwenhuyze, W., et al. (2014). Changes in Holocene climate and the intensity of Southern Hemisphere westerly winds based on a high-resolution palynological record from sub-Antarctic South Georgia. *The Holocene*, *25*, 263–279.

Stuiver, M., & Pollach, H. (1977). Reporting of ^{14}C data. *Radiocarbon*, *19*(3), 355–363. https://doi.org/10.1017/S0033822200003672

Subt, C., Yoon, H. I., Yoo, K. C., Lee, J. I., Leventer, A., Domack, E. W., & Rosenheim, B. E. (2017). Sub-ice shelf sediment geochronology utilizing novel radiocarbon methodology for highly detrital sediments. *Geochemistry, Geophysics, Geosystems*, *18*, 1404–1418. https://doi.org/10.1002/2016GC006578

van Beek, P., Reyss, J. L., Paterne, M., Gersonde, R., van der Loeff, M. R., & Kuhn, G. (2002). ^{226}Ra in barite: Absolute dating of Holocene Southern Ocean sediments and reconstruction of sea-surface reservoir ages. *Geology*, *30*, 731–734.

van der Bilt, W. G. M., Bakke, J., Werner, J. P., Paasche, O., Rosqvist, G., & Solheim Vatle, S. (2017). Late Holocene glacier reconstructions reveals retreat behind present limits and two-stage little ice age on subantarctic South Georgia. *Journal of Quaternary Science*, *32*(6), 888–901. https://doi.org/10.1002/jqs.2937

Van der Putten, N., & Verbruggen, C. (2005). The onset of deglaciation of Cumberland Bay and Stromness Bay, South Georgia. *Antarctic Science*, *17*(1), 29–32. https://doi.org/10.1017/S0954102005002397

Vonk, J. E., Semiletov, I. P., Dudarev, O. V., Eglinton, T. I., Andersson, A., Shakhova, N., et al. (2014). Preferential burial of permafrost-derived organic carbon in Siberian-Arctic shelf waters. *Journal of Geophysical Research: Oceans*, *119*, 8410–8421. https://doi.org/10.1002/2014JC010261

Wacker, L., Bonani, G., Friedrich, M., Hajdas, I., Kromer, B., Němec, M., et al. (2010). MICADAS: Routine and high-precision radiocarbon dating. *Radiocarbon*, *52*(2), 252–262. https://doi.org/10.1017/S0033822200045288

Wacker, L., Fahrni, S. M., Hajdas, I., Molnar, M., Synal, H.-A., Szidat, S., & Zhang, Y. L. (2013). A versatile gas interface for routine radiocarbon analysis with a gas ion source. *Nuclear Instruments and Methods in Physics Research B*, *294*, 315–319. https://doi.org/10.1016/j.nimb.2012.02.009

Wacker, L., Fülöp, R. H., Hajdas, I., Molnár, M., & Rethemeyer, J. (2013). A novel approach to process carbonate samples for radiocarbon measurements with helium carrier gas. *Nuclear Instruments and Methods in Physics Research B*, *294*, 214–217. https://doi.org/10.1016/j.nimb.2012.08.030

Welte, C., Hendriks, L., Wacker, L., Haghipour, N., Eglinton, T. I., Günter, D., & Syal, H.-A. (2018). Towards the limits: Analysis of micro scale ^{14}C samples using EA-AMS. *Nuclear Instruments and Methods in Physics Research B*, *437*, 66–74. https://doi.org/10.1016/j.nimb.2018.09.046

White, D. A., Bennike, O., Melles, M., & Berg, S. (2018). Was South Georgia covered by an ice cap during the last glacial maximum? In: Siegert MJ, Jamieson SSR, White DA (eds.) exploration of subsurface Antarctica: Uncovering past changes and modern processes. *Geological Society, London, Special Publications*, *461*(1), 49–59. https://doi.org/10.1144/SP461.4

Winterfeld, M., Mollenhauer, G., Dummann, W., Köhler, P., Lembke-Jene, L., Meyer, V. D., et al. (2018). Deglacial mobilization of pre-aged terrestrial carbon from degrading permafrost. *Nature Communications*, *9*(1). https://doi.org/10.1038/s41467-018-06080-w

Yamane, M., Yokoyama, Y., Miyairi, Y., Suga, H., Matsuzaki, H., Dunbar, R. B., & Ohkouchi, N. (2014). Compound-specific ^{14}C dating of IODP expedition 318 core U1357A obtained off Wilkes Land coast, Antarctica. *Radiocarbon*, *56*, 1–9.

Yokoyama, Y., Anderson, J. B., Yamane, M., Simkins, L. M., Miyairi, Y., Yamazaki, T., et al. (2016). Widespread collapse of the Ross ice shelf during the late Holocene. *PNAS*, *113*(9), 2354–2359. https://doi.org/10.1073/pnas.1516908113